





# Prediction of mine drainage generation potential and the prevention method of the groundwater pollution in the Gümüşköy (Kütahya) mineralization area, NW Turkey

**Selcuk ALEMDAG\***  <https://orcid.org/0000-0003-2893-3681>;  e-mail: selcukalemdag@gmail.com

**Enver AKARYALI**  <https://orcid.org/0000-0003-1495-9186>; e-mail: eakaryali@gmail.com

**Mehmet Ali GÜCER**  <https://orcid.org/0000-0002-9075-3350>; e-mail: maligucer@gmail.com

\* Corresponding author

Department of Geological Engineering, Faculty of Engineering and Natural Sciences, Gümüşhane University, Gümüşhane 29100, Turkey

**Citation:** Alemdag S, Akaryali E, Gücer MA (2020) Prediction of mine drainage generation potential and the prevention method of the groundwater pollution in the Gümüşköy (Kütahya) mineralization area, NW-Turkey. *Journal of Mountain Science* 17(10). <https://doi.org/10.1007/s11629-020-6124-1>

© Science Press, Institute of Mountain Hazards and Environment, CAS and Springer-Verlag GmbH Germany, part of Springer Nature 2020

**Abstract:** One of the leading factors of seepage contamination is mine drainage, which creates serious ecological risks on the environment both during operation and post-mining times. In this study, experimental processes have been carried out to determine the occurrence of mine drainage in the Gümüşköy (Kütahya) mineralization area (Northwest Turkey). The prevention method for potential mine drainage occurrence has been also discussed. High enrichment was observed which are directly related to mineralization in trace element concentrations, especially in potentially toxic metals such as Ag, Cd, Mo, Ba, Bi, and Zn. Based on short-term tests, mine drainage formation has not been expected according to the pH (7.36-9.38), contact leaching, and acid-base accounting studies. However, in the long-term, acid generation potential has been expected because of weathering and oxidation in terms of rock type and mineralization in the area. Therefore, in order to prevent groundwater contamination in the event of a possible formation of mine drainage, the hydraulic conductivity of the stock area bedrock was evaluated by the in situ tests performed in the field and it was found to be moderately permeable ( $K=1.9 \times 10^{-6}$  m/s). In order to make the stock area bedrock impermeable,

natural clay will be laid and compressed at the base of the stock area. When the finite elements were modeled by seepage analysis, the seepage discharge to be formed on the base rock at a depth of 5 m was determined as  $3.17 \times 10^{-19}$  m<sup>3</sup>/s. Since the discharge value determined in the seepage analysis after modeling is very close to zero, contamination of possible ground and surface water will be prevented.

**Keywords:** Ecological risks; Environmental assessment; Mine drainage; Seepage analysis

## Introduction

The acid mine drainage (AMD) is defined as the occurrence of chemical oxidation by reacting with air (oxygen) and water of sulfur bearing minerals such as pyrite, chalcopyrite, pyrrhotite sphalerite etc., under atmospheric conditions, sometimes with the contribution of microbiological organisms e.g., *Acidophilic bacterium*, *Acidithiobacillus ferrooxidans* (Mills 1995; EPA 1994a, b; Skousen et al. 2000; Betrie et al. 2015; Liu et al. 2017; Jia et al. 2018). When the sulfur bearing minerals react with water and oxygen during the mining activities or after the mine

**Received:** 05-Apr-2020

**1<sup>st</sup> Revision:** 19-Jun-2020

**2<sup>nd</sup> Revision:** 30-Jul-2020

**Accepted:** 18-Aug-2020

operation, some heavy metals (Fe, Pb, Cu, Zn, etc.) dissolve and give acidic character to the drainage water and, it causes the formation of acid mine drainage (Skousen et al. 2000; Morin and Hutt 2001; Akçil and Koldaş 2006; Akaryalı et al. 2018; Alemdağ et al. 2020). The characteristic ore deposit types including porphyry copper, volcanogenic massive sulphide, high-sulfidation epithermal and skarn deposits are most commonly associated with acid mine drainage. A number of studies in recent years have been carried out on the kinetics of pyrite oxidation in both biotic and abiotic systems (e.g., Singer and Stumm 1970; Boon and Heijnen 1998; Holmes and Crundwell 2000; Descostes et al. 2004; Bouffard et al. 2006; Gleisner et al. 2006; Brunner et al. 2008; Ma and Lin 2013; Liu et al. 2017; Jia et al. 2018). Kalyoncu Ergüler and Ergüler (2020) conducted kinetic column tests by separating the materials they obtained from field studies into different dimensions and determined that the key parameters controlling the acid production rate were time and pH. Alemdağ et al. (2020) evaluated the Acid Producing Potential of Flotation Facility Wastes and laid 50cm clay to ensure impermeability at the dam floor where wastes will be stored. Then, the resulting cross-section model was evaluated by the finite element method and possible infiltration conditions were analyzed.

Accumulation of sulphide ores produced from mining sites operated by an open pit or underground method in areas open to atmospheric effects may lead to pollution of groundwater resources and environmental problems (e.g., Kim et al. 2017). There are many methods to prevent the occurrence of possible mine drainage in field studies from past to present. It is possible to sort the most common of these methods as below.

Firstly, the area around the mine site should be surrounded by a drainage channel so that the water flowing due to the seasonal rainfall does not enter the stock area. Second, limestone filling should be applied on the bottom or drainage channels for the neutralization of the mine drainage formed by ore mass to be deposited in the stockpile (Rötting et al. 2008; Caraballo et al. 2009; Delibalta et al. 2016).

In addition to these, passive and active treatment methods are used to prevent possible AMD formation. Passive treatment methods are

listed as natural and artificial marshes, anoxic limestone drains, systems producing sequential alkali, limestone pools, open limestone channels and the use of anaerobic and aerobic wetlands which are known to considerably treat mineral waters (Berghorn and Hunzeker 2001; Marchand et al. 2010; Lottermoser and Ashley 2011). Active treatment is carried out with the chemicals selected for use in the purification process (EPA 1983). With these applications, groundwater contamination is prevented and surface water contamination can be treated.

In this study, except for the currently applied methods, the permeability characteristics of the bedrock of the ore deposit area were determined, and if the base rock is permeable, it will be rendered impermeable by various methods. This method has previously been applied by several researchers (Gurocak and Alemdağ 2012; Alemdağ 2015; Kanik and Ersoy 2019) in the dams built for the storage of mineral waste and energy generation.

In open pit mine operation system, when the pH of mine water is raised by fresh water or neutralizing minerals, soluble metals such as Fe<sup>2+</sup> ions are oxidized and a yellow-orange iron (oxy) hydroxides are precipitated. During the mine operation in ore deposit and stockpile area, oxidation of sulfur minerals with external effects causes acidic water formation and mine drainage is developed.

In this study, it is aimed to store the ore products extracted from Gümüşköy Ag-Pb-Zn deposit in the stock area and to evaluate the potential AMD hazard. For this purpose, natural clay was laid and compacted at the base of the stock area to prevent environmental pollution caused by seepage waters. This method was applied for the first time to prevent the permeability of the stock area and to evaluate the mass permeability after the application, the stock area was modeled by the seepage analysis and the control of the improvement made by determining the leakage discharges at a depth of 5 m from the surface.

In addition to these, acidic waters will be collected in the upper drainage collection pool by drainage systems to be formed on the clay layer planned to be laid on the floor of the stockpile. Afterward, neutralization of AMD acidity will be achieved with precipitation tanks containing chemicals such as CaCO<sub>3</sub>, Ca(OH)<sub>2</sub>, Na<sub>2</sub>CO<sub>3</sub> to

remove Fe, Mn, and other metal deposits.

## 1 Geological Setting

Turkey was geologically composed during the Alpine orogeny in which mostly ophiolites and metamorphics are related tectonically. It was formed by the collision of Gondwana with Laurasia in the Late Tertiary (Şengör and Yılmaz 1981; Şengör et al. 1985). There are several micro-plates or terranes depending on the geological and tectonic features (Figure 1a; Okay and Tüysüz 1999) such as Arabian platform and terranes (the Sakarya Composite Terrane, the Istanbul-Zonguldak Terrane and the Anatolide-Tauride Terrane) from south to north, respectively. The Istanbul-Zonguldak and the Sakarya Composite Terranes is separated by the Intra-Pontide Suture Belt in the north (e.g., Çimen et al. 2016). However, the Izmir-Ankara-Erzincan Suture Belt, which stretches from the Aegean Sea to the Lesser Caucasus, represents a boundary between the Sakarya Composite and the Anatolide-Tauride Terranes (e.g., Aldanmaz et al. 2008; Parlak et al. 2013; Gücer et al. 2016, 2019; Çimen et al. 2017, 2018; Çimen and Öztüfekci 2018; Çimen 2019).

The Tavşanlı zone is located south of the Izmir-Ankara-Erzincan suture belt and it corresponds to the remnant of the major Neotethys ocean, which separated Laurasia and Gondwana from the Triassic to Cretaceous or early Tertiary (Tekin et al. 2002; Meijers et al. 2010; Lefebvre et al. 2013; Plunder et al. 2013). There are numerous and different types of mineral deposits in the region, including porphyry (e.g., Ag, Au, Pb, Zn, Cu), skarn and epithermal deposits associated with tectonism and magmatism/volcanism (e.g., Vıcıl 1982; Arık 2002; Yıldız 2007; Arık and Yıldız 2010; Arık 2012 and references therein). The study area is located in the Gümüşköy (Kütahya) between Tavşanlı and Afyon zones. The various rock types are exposed in the area ranging from Paleozoic to Pliocene in age (Figure 1b). The basement unit consists of low-grade metamorphic rocks of the Carboniferous-Permian Şahin Formation (Arık 2002, 2012). They are composed of widespread schists, phyllite, meta-sandstone, meta-conglomerate, meta-carbonate and quartzite. These metamorphic rocks are overlain unconformably by the Tertiary volcano sedimentary sequence

(Tavşanlı volcanics and Emet formation), as well as Upper Cretaceous Melange with tectonically. The Tavşanlı volcanics generally composed of rhyolitic and rhyodacitic tuffs, whereas Emet formation consist of limestone and dolomitic limestones. Also, the presence of various Sb-As-Ag-Pb-Zn enrichments in the study area was reported related to the Cenozoic volcanic activities (e.g., Ziegler 1960; Vıcıl 1982; Yiğitgüden 1984; Arık 2002, 2008, 2012; Şaşmaz et al. 2016; Yıldırım and Şaşmaz 2017).

In the ore deposit area, host rocks consist of marl intercalated with limestone, claystone, sandstone, conglomerate and tuffs (Çökköy Formation); marl intercalated with clayey and/or cherty limestone (Emet Formation); schists, quartzites, marbles and meta-sandstones (Figure 2). Furthermore, the presence of limestone and dolomite is the most important factor that increases the neutralization potential.

The ore deposit area is exploited by the open-pit mining method. The minimum thickness of the ore deposit is 2.5 m and the maximum thickness is about 41 m. The mineralization occurs in the schists and silicified tuff zones. Ore mineral assemblages consist of silver minerals such as pyrargyrite, argentite, and base metal sulfides such as sphalerite, galena, chalcopyrite, etc. The grade of Ag ore ranges from 55 mg/L to 300 mg/L, and the average tenor is 133 mg/L. Also, gangue minerals and type of alterations are mainly represented by dolomite, quartz and calcite, hematitic, limonitic and siliceous, respectively.

## 2 Materials and Methods

### 2.1 Sampling

Twelve samples from the ore-bearing rocks and ten samples from host rocks and stock areas were collected in the study area (Figure 3). The sampling of the ore-bearing, especially silver (Ag) and zinc (Zn) bearing rocks were taken from systematically the ore vein depending on mineral compositions. The host rocks and stock area samples were compiled homogeneously in the study area, particularly from the limestone, dolomite, quartzite, and schist.

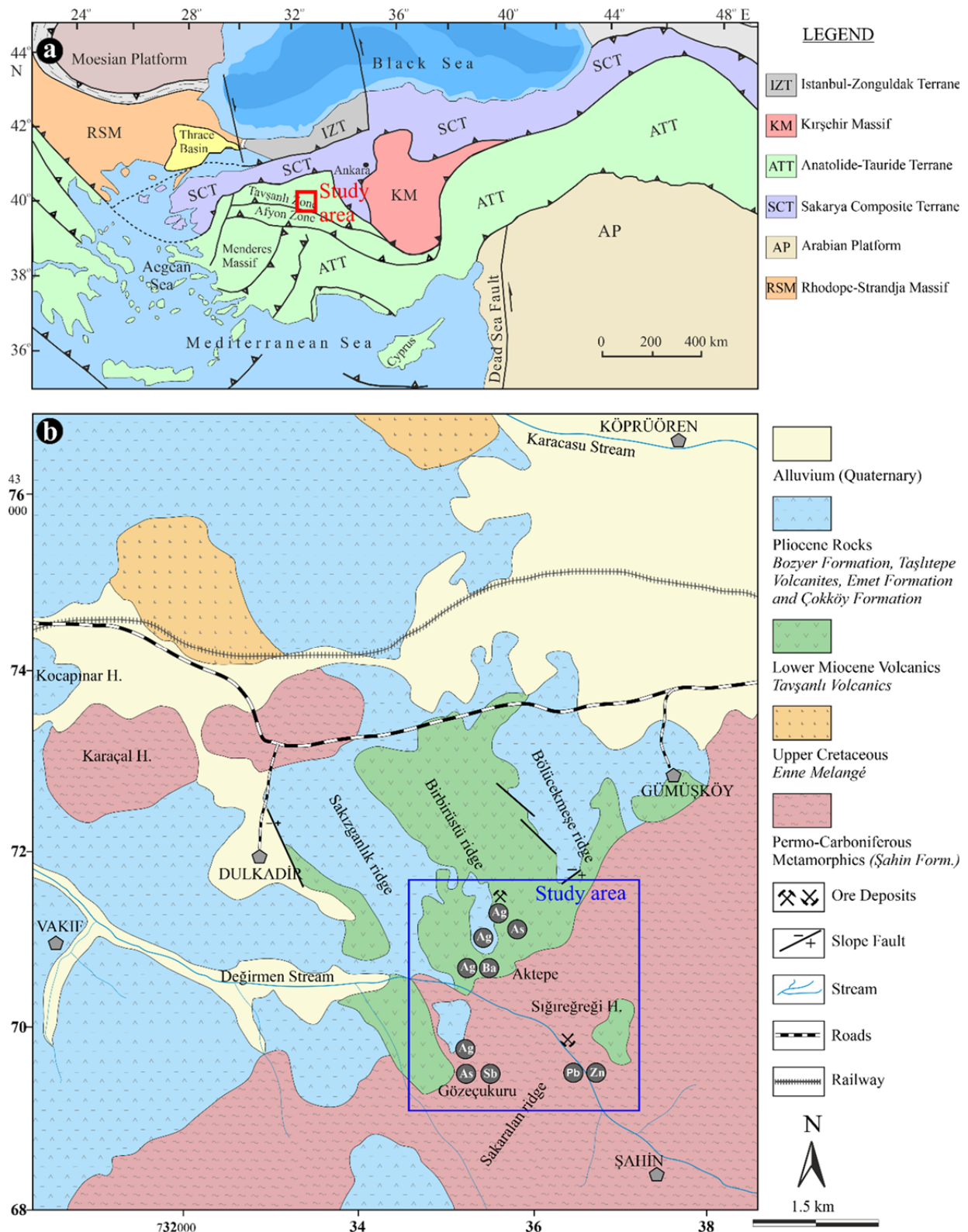


**Figure 1** (a) Map of the main tectonic units of Turkey (simplified from Okay and Tüysüz 1999). (b) Geological map (modified from Arık and Yıldız 2010; Şaşmaz et al. 2016; Yıldırım and Şaşmaz 2017) and location of the study area.

## 2.2 Whole-rock geochemical analysis

The geochemical analyses of 12 host rocks and 10 ore-bearing samples were performed in SGS

Analytical Laboratories, Dilovasi, Kocaeli (Turkey). Major oxide and trace element compositions were determined by inductively coupled plasma atomic emission spectroscopy (ICP-AES). Besides, precious metals such as Ag and Zn were determined with atomic absorption spectrometry (AAS). Samples were crushed into small chips of 0.1-1 cm using a jaw crusher and then powdered using a mild-steel mill. For major elements, samples were prepared with 0.2 g of rock powder fused with 1.5 g LiBO<sub>2</sub>. Carbon (C; 2%) and sulfur (S; 1%) standards were prepared for carbon dioxide and sulfur measurements. Loss on ignition (LOI) is defined as the difference in weight before and after ignition at 1000°C. The detection limits are approximately 0.01 to 0.1 wt% for major oxides and 0.1 to 10 mg/L for trace elements.

### 2.3 Leaching tests

Contact Leachate Tests in 22 representative ore-bearing and rock samples were carried out at Gümüşhane University, Laboratory of the Department of Food Engineering of the Faculty of Engineering and Natural Sciences. The analyses were performed according to the “modified US EPA (The United States Environmental Protection Agency) 1312” standard. The samples were subjected to 3:1 liquid/solid ratio of pure water (deionized) contact leachate test for 24 hours. In addition, during the analyzes, in order to prevent precipitation, 2% nitric acid (HNO<sub>3</sub>) solution was prepared from nitric acid 65% Suprapur, and one drop was added to the water samples. Trace

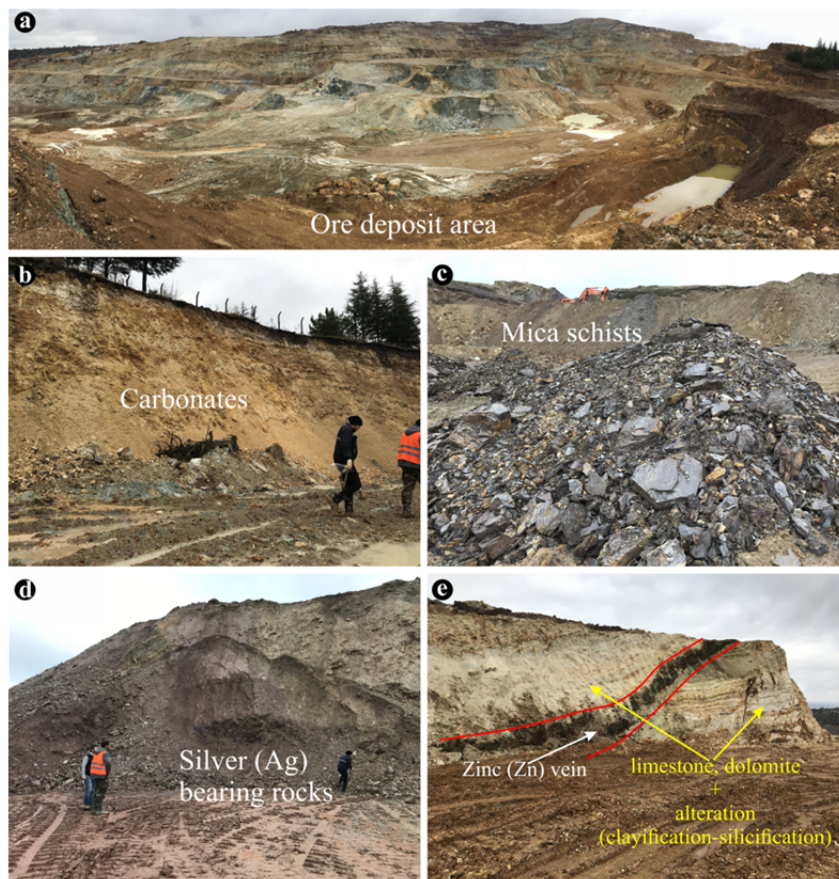


**Figure 2** Field photographs of ore-bearing and related rocks from the study area. (a) Panoramic view of the ore deposit area. (b) The carbonate rocks (limestone/dolomite, etc.) where zinc (Zn) mineralization is observed generally. (c) Low grade micaschists. (d) Silver (Ag) stockpile area. (e) Zinc (Zn) mineralization and related limestone-dolomite rocks.

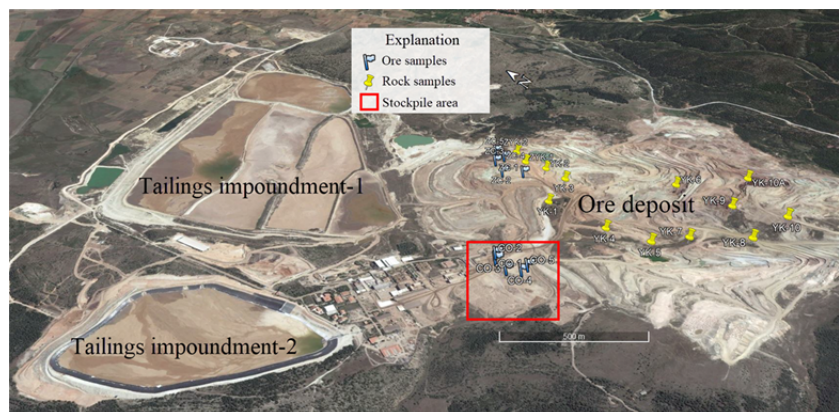


**Figure 3** Google Earth image of the study area, and distribution of ore-bearing samples (yellow pin) and host rock (blue flags) samples. Source: Google Earth, accessed in 2018.

element concentrations were determined with Agilent 7700 inductively coupled plasma mass spectrometer (ICP-MS).

## 2.4 Acid-Base Accounting (ABA) tests

The ABA tests were performed in SGS Dilovasi (Kocaeli, Turkey) Chemical Products and Vernolab Laboratories. Besides, the concentrations and neutralization potential (NP) of carbonate were determined in all samples. Paste pH analysis was carried out according to the MEND (2009) standard. Moreover, MEND project 1.20.1 (MEND 2009) standards were used for NP, acid production potential (AP) and net neutralization potential (NNP) analysis. If the NNP is greater than 20 kg/t CaCO<sub>3</sub>, it is generally accepted that the material is non-acid producing, and the NNP is less than -20 kg/t CaCO<sub>3</sub>, it is generally accepted that the material is acid producing (Ferguson and Morin 1991; Miller et al. 1991). NNP values between -20 and 20 kg/t CaCO<sub>3</sub> are in range of uncertainty, and kinetic tests may be needed (Ferguson and Morin 1991; Miller et al. 1991). In addition, total sulphur (%), acid leachable SO<sub>4</sub>-S (%), sulphide (%), total carbon (%) and carbonate (%) analyses were performed according to the “ASTM E1915-07A” standard. NP and AP values were calculated from  $[50 \times (N \text{ of HCl} \times \text{total HCl added} - N \text{ NaOH} \times \text{NaOH added})]$  and  $[\% \text{ Sulphide-Sulphur} \times 31.25]$  (Sobek et al. 1978) formulas, respectively. The most used method to estimate AP is based on the sulfur content and it is calculated by multiplying the sulphide-S content (wt%) by a factor of 31.25 (Sobek et al. 1978; Lawrence and Wang 1996; Lawrence and Scheske 1997; Frostad et al. 2003).

## 2.5 Engineering applications and experiments

In order to determine the aquifer characteristics (T: Transmissibility, K: Hydraulic Conductivity) of the stockpile basement rock, pumping results in the drilled well were evaluated according to three different methods (Jacob, Theis, Neuman). In the calculations, the Jacob graphic method, Aquifer Win32, and Aquifer Test Pro computer programs were used. The hydraulic conductivity coefficient obtained as a result of these studies will be used as an input parameter in the modeling of the stock area by numerical analysis method. In determining the material properties of the stock area foundation rock, the test methods recommended by ISRM (2007) were

used in the core samples compiled from the drilled wells and unit volume weight, uniaxial compressive strength, elasticity module parameters were determined. To determine the rock mass constants (mb, s, a), the geological strength index (GSI), rock material constant (mi), uniaxial compressive strength and trauma factor (D) parameters of the rock mass were determined using the RS2 (Rocscience 2019) computer program. In the RS2 numerical analysis program, Hoek et al. (2002) proposed Generalized Hoek – Brown criterion was used. The seepage of the stockpile area was analyzed using the RS2 software (Rocscience 2019). The Seepage behavior of the material in two-dimensional Groundwater Steady State FEA conditions was modeled using Finite Element Groundwater Seepage. The rock mass environment was chosen as plastic and isotropic. A graded and six-node triangular finite element mesh was used in the stockpile area seepage model. To Modeling, in addition, the discharge section plane was added to determine the steady-state volumetric flow rate that will occur in the rock mass. The properties of natural compressed clay to be laid on the floor to ensure impermeability in the stock area were determined, and the minimum thickness should be 30 cm.

## 3 Results and Discussion

### 3.1 Ore and host rock geochemistry

Representative whole rock major and trace element analyses of the ore bearing and host rocks from the mineralization area are given in Table 1 and Table 2. The major element contents of the ore-bearing samples generally have values close to or below the average composition of continental crust (ACC: Yaroshevsky 2006). SiO<sub>2</sub>, TiO<sub>2</sub>, MgO, MnO and CaO contents were higher than the ACC (Figure 4a). The contents of the SiO<sub>2</sub> and Al<sub>2</sub>O<sub>3</sub> in the rocks have a wide-ranging from 21.30 to 69.10 wt% and from 2.78 to 14.20 wt%, respectively. In addition, they have high P<sub>2</sub>O<sub>5</sub> composition up to 13.30 wt%. However, MgO, MnO and CaO vary between 0.72-10.50 wt%, 0.52-1.72 wt% and 1.95-20.90 wt%, respectively. MnO enrichment in ore-bearing samples could be related to the chemical composition of the ore minerals in the study area.

**Table 1** Representative major oxide (wt%) composition of the ore-bearing samples and host rocks from mineralization area

Major oxide	SiO <sub>2</sub>	Al <sub>2</sub> O <sub>3</sub>	TiO <sub>2</sub>	Fe <sub>2</sub> O <sub>3</sub>	MgO	MnO	CaO	Na <sub>2</sub> O	K <sub>2</sub> O	P <sub>2</sub> O <sub>5</sub>	Cr <sub>2</sub> O <sub>3</sub>	V <sub>2</sub> O <sub>5</sub>	LOI*	Total
Detection limit	0.01	0.01	0.01	0.01	0.01	0.01	0.01	0.01	0.01	0.01	0.01	0.01		
ACC**	57.76	15.12	0.83	7.15	3.48	0.12	4.12	3.24	3.13	0.23	0.03	0.019		
Sample	Host rocks (limestone, dolomite, quartzite and schist)													
ZYK-1	63.50	13.00	0.08	0.64	0.84	0.01	2.20	0.85	4.58	0.14	UDL	UDL	9.66	95.50
ZYK-2	62.10	14.60	0.11	0.51	0.25	UDL	0.73	1.46	9.73	0.04	UDL	UDL	5.14	94.60
YK-2	92.30	0.34	UDL	0.63	1.03	0.05	1.87	0.11	0.18	0.09	0.01	UDL	3.33	100.00
YK-3	16.40	0.34	UDL	0.54	15.90	0.40	27.10	0.12	0.13	0.06	UDL	0.01	38.80	99.70
YK-4	59.90	18.00	0.78	8.04	0.91	0.19	0.29	0.34	5.05	0.13	0.01	0.03	4.85	98.50
YK-5	62.30	18.20	0.83	6.11	0.91	0.07	0.39	0.37	5.01	0.18	0.01	0.03	4.73	99.10
YK-6	60.70	17.00	0.79	8.47	0.85	0.29	0.37	0.41	4.75	0.19	0.01	0.02	4.90	98.70
YK-7	55.40	21.00	0.88	7.82	1.04	0.04	0.23	0.37	5.96	0.23	0.01	0.04	5.80	98.90
YK-8	60.20	17.80	0.76	9.19	1.01	0.20	0.14	0.26	5.52	0.08	0.01	0.02	3.87	99.10
YK-9	61.60	18.30	0.79	6.78	0.92	0.10	0.41	0.36	5.08	0.19	0.01	0.03	4.98	99.60
YK-10	61.50	18.00	0.82	7.19	0.92	0.28	0.38	0.34	5.12	0.19	0.01	0.02	4.44	99.10
YK-10A	42.90	6.18	0.03	1.09	7.56	0.16	9.87	0.20	0.14	0.82	UDL	UDL	18.70	87.70
Minimum	16.40	0.34	0.08	0.51	0.25	0.01	0.14	0.11	0.13	0.04	0.01	0.01	3.33	
Maximum	92.30	21.00	0.88	9.19	15.90	0.40	27.10	1.46	9.73	0.82	0.04	0.04	38.80	
Average	57.68	13.15	0.57	4.77	3.45	0.17	5.09	0.48	4.37	0.23	0.02	0.03	10.81	
Sample	Ore-bearing samples													
ZC-1	26.60	6.46	0.23	6.96	5.25	1.31	8.37	2.12	1.42	0.24	UDL	0.01	17.00	75.90
ZC-2	21.30	2.78	0.10	3.67	9.60	1.72	15.90	1.83	1.01	0.31	UDL	UDL	25.20	83.40
ZC-3	62.10	3.17	0.04	7.48	1.23	0.90	1.95	2.44	0.95	0.18	UDL	UDL	6.27	86.70
ZC-4	31.00	5.90	0.06	3.46	0.73	0.64	20.90	2.45	4.20	13.30	UDL	UDL	6.29	89.00
ZC-5	45.40	11.00	0.39	8.33	1.89	1.04	3.22	2.64	1.66	0.13	UDL	UDL	11.30	87.00
CO-1	69.10	12.20	3.79	1.25	1.34	0.88	3.88	0.58	0.16	0.10	0.01	0.02	4.51	97.90
CO-2	63.60	12.30	4.49	1.68	1.87	0.52	4.30	0.53	0.16	0.25	UDL	0.03	5.96	95.60
CO-3	51.20	10.10	4.00	2.11	10.50	0.88	3.29	0.45	0.15	0.20	UDL	0.01	12.70	95.60
CO-4	63.30	14.20	5.16	0.93	0.72	0.80	4.76	0.65	0.17	0.13	UDL	0.03	4.88	95.70
CO-5	63.00	11.30	4.07	2.09	2.85	0.61	4.45	0.48	0.11	0.18	UDL	0.02	6.61	95.80
Minimum	21.30	2.78	0.04	0.93	0.72	0.52	1.95	0.45	0.11	0.10		0.01	4.88	
Maximum	69.10	14.20	5.16	8.83	10.50	1.72	20.90	2.64	4.20	13.30		0.03	25.20	
Average	49.66	8.94	2.23	3.80	3.60	0.93	7.10	1.42	1.00	1.50		0.02	10.07	

**Note:** \*LOI: Loss on ignition, \*\*ACC: Average composition of continental crust. UDL: Under Detection Limit. The orange-colored values represent the values above ACC. Italicized numbers represent the minimum, maximum and average of the samples for each major oxide parameter.

Similarly, high CaO content is related to carbonate host rocks (limestone, dolomite, marl, etc.) which contain mineralization in the field.

In the host rocks, SiO<sub>2</sub>, Al<sub>2</sub>O<sub>3</sub> and CaO values ranged between 16.40 - 92.30 wt%, 0.34-21.00 wt% and 0.14-27.10 wt%, respectively. In addition, FeO and K<sub>2</sub>O values vary from 0.51-9.19 wt% and 0.13-9.73 wt%. The wide range of major oxide contents in the samples is associated with the different host rock types such as limestone, dolomite, marl, quartzite, schist. Generally, there are increases in SiO<sub>2</sub>, Al<sub>2</sub>O<sub>3</sub>, FeO, MnO and K<sub>2</sub>O contents in comparison with the ACC for studied samples (Figure 4b). According to compared ACC, the high K<sub>2</sub>O and partly high CaO values in the host rocks are related to the hydrothermally altered minerals such as sericite and plagioclase, respectively.

The trace element distributions of both host rocks and ore-bearing samples exhibit a higher enrichment compared to the ACC (Table 2). In the

ore deposit area, there were high enrichments of Ag, As, Ba, Bi, Cd, Mo, Sb, S, W and Zn element contents in all samples. In the ore-bearing samples Ag, As, Mo, Sb, S and Zn compositions vary from 5.1-71 mg/L, 700-30000 mg/L, 1.3-7.6 mg/L, 359-5365 mg/L, 480-7800 mg/L to 5032-74390 mg/L (Figure 4c), whereas in the host rocks ranged between 2.6-47 mg/L, 280-67000 mg/L, 0.2-404 mg/L, 119-2618 mg/L, 200-4600 mg/L and 955-12517 mg/L (Figure 4d), respectively. Consequently, effect of the mineralization in the major oxides is observed insignificantly, and the various distributions in the elemental concentration indicate different mineralogical compositions. However, high enrichment in trace element concentrations, especially in heavy metals such as Ag, Mo, Zn is directly related to mineralization at the ore deposit area.

### 3.2 Assessment of contact leaching tests

**Table 2** Representative trace element (mg/L) composition of the ore-bearing samples and host rocks from mineralization area.

Trace element	Ag	As	Ba	Bi	Cd	Cu	Mo	Sb	Sr	S	Th	W	Zn	Zr
ACC*	0.07	1.7	650	0.009	0.13	47	1.1	0.5	340	470	13	1.3	83	170
Sample	Host rocks (limestone, dolomite, quartzite and schist)													
ZYK-1	2.6	5700	9000	0.63	256	100	5.8	2618	2382	890	53	6.5	12517	42
ZYK-2	47	3400	8000	0.3	99	121	1.8	1074	156	4600	21	4.3	11300	100
YK-2	4.8	1200	420	UDL	9.4	28	1	227	85	200	2.1	0.6	1790	77
YK-3	3.9	1000	240	UDL	56	55	1.3	172	858	1100	18	1.9	955	39
YK-4	12	450	4800	0.39	19	30	0.5	172	42	930	21	5.7	5056	74
YK-5	17	280	750	0.14	8.1	12	0.3	136	21	UDL	4.6	4.9	6127	61
YK-6	19	770	1200	0.20	36	33	0.7	208	33	UDL	28	7.6	7237	54
YK-7	10	1000	1800	0.45	15	70	1.4	119	36	UDL	6.5	2.4	4344	70
YK-8	12	530	1600	0.29	20	35	1.1	263	31	300	13	6.6	2503	74
YK-9	11	320	800	0.25	11	26	0.2	145	24	UDL	9	5.1	6167	57
YK-10	17	300	950	0.28	6.8	12	404	167	32	790	29	7.5	5385	75
YK-10A	42	67000	16000	UDL	11	48	3.3	1493	1763	1500	6.9	1.7	2390	40
Minimum	2.6	280	240	0.2	6.8	12	0.2	119	21	200	2.1	0.6	955	40
Maximum	47	67000	16000	0.63	256	121	404	2618	2382	4600	53	7.6	12517	100
Average	16.53	6829	3797	0.33	45.61	47.50	35.12	566.17	455.25	1288.75	17.68	4.57	5481	64
Sample	Ore-bearing samples													
ZC-1	71	22000	24000	0.18	591	93	3.4	3464	667	7800	25	9.8	52348	62
ZC-2	23	6200	25000	UDL	138	31	7.6	2621	428	3400	6.7	1.8	21074	40
ZC-3	9.4	30000	4600	0.11	360	29	7.3	5365	274	480	13	7.3	66551	68
ZC-4	10	25000	2400	0.22	570	15	5.7	1950	2682	2500	26	9.1	50507	240
ZC-5	5.1	23000	7800	0.42	548	23	4.6	1879	164	550	16	10	74390	130
CO-1	48	700	2700	0.34	32	78	1.5	359	71	870	20	6.4	5032	60
CO-2	49	2300	12000	0.36	83	155	5.3	955	155	3700	23	4.0	7227	90
CO-3	46	3200	12000	0.29	32	106	2.1	764	238	3700	19	4.0	6671	68
Co-4	23	3000	5500	0.32	72	96	1.3	836	87	2200	5.3	6.5	17145	75
CO-5	47	3400	8000	0.30	99	121	1.8	1074	156	4600	21	4.3	11300	100
Minimum	5.1	700	2400	0.11	32	15	1.3	359	71	480	5.3	1.8	5032	40
Maximum	71	30000	25000	0.42	591	155	7.6	5365	2682	7800	26	9.8	74390	240
Average	33.15	11880	10400	0.282	252.5	74.7	4.06	1926.7	492.2	2980	17.5	6.32	31225	93

**Note:** \*ACC: Average composition of continental crust. UDL: Under detection limit. The orange-colored values represent the values above ACC. Italicized numbers represent the minimum, maximum, and average of the samples for each trace element parameter.

In the mine and stockpile areas, contact leach tests were implemented for the assessment of acid drainage formation and the results are given in Table 3. Also, the samples were compared with quality classification of the intra-continental water resources suggested by RG28483 (2012).

The pH values of the ore-bearing samples varied between 7.94-8.47, while the host rocks pH value range was between 7.65-9.10. The obtained pH results indicated an alkaline environment. The pH values of the samples were determined to be first-class quality according to the quality classification of the intra-continental water resources. Although there are no geochemical anomalies for Cd, Co, Cr and Cu elements in ore-bearing samples, there is an increase in Fe, Mn, Ni, Pb and Zn elements (Figure 5a). The Fe, Pb and Zn values are respectively between 0.01-0.60 mg/L, 0.10-0.14 mg/L and 0.04-0.44 mg/L, and these distributions are related to the mineralization in

the study area. Similarly, there are no geochemical anomalies for Cd, Co, Cr and Cu concentrations in the host rocks, whereas the significant enrichment in Fe and Zn contents (Figure 5b). Fe and Zn contents are between 0.001-2.04 mg/L and 0.015-1.37 mg/L, respectively. The increase of Fe contents in both ore-bearing samples and host rocks indicated the effects of hydrothermal alteration.

The influence of climatological conditions, host rocks, alterations and mining process on the nature of the acid rock/mine drainage can be illustrated using Ficklin diagrams. These diagrams developed by Plumlee et al. (1992) to help interpret variations in rock/mine drainage water chemistry between different deposit types based on the pH values and the sum of the base metals (Zn+Cu+Cd+Pb+Co+Ni). The studied samples are characterized by low Cd, Co, Cr, and Cu concentration, whereas having high pH (7.65-9.00) and Zn, Pb, and Ni values. In the Ficklin



discrimination diagrams (Figure 6a), samples fall into the mostly “near-neutral/low-metal” and to a lesser extent “near-neutral/high-metal” fields. These indicated that the studied rocks have neutral mine drainage characteristic. Moreover, Ficklin diagrams can be used to describe some principles that manage mine water quality. As shown in the Figure 6b, increasing in pyrite content tends to

result in more acidic, whereas an increase in carbonate content tends to lead to more alkaline waters. Also, increasing in base metal sulphide content tends to result in an increase in trace metal concentrations. In Figure 6b, the studied rocks are typically characterized by “dilution by surface water” contents. This less acidic and concentrated character of the samples indicates that the greater

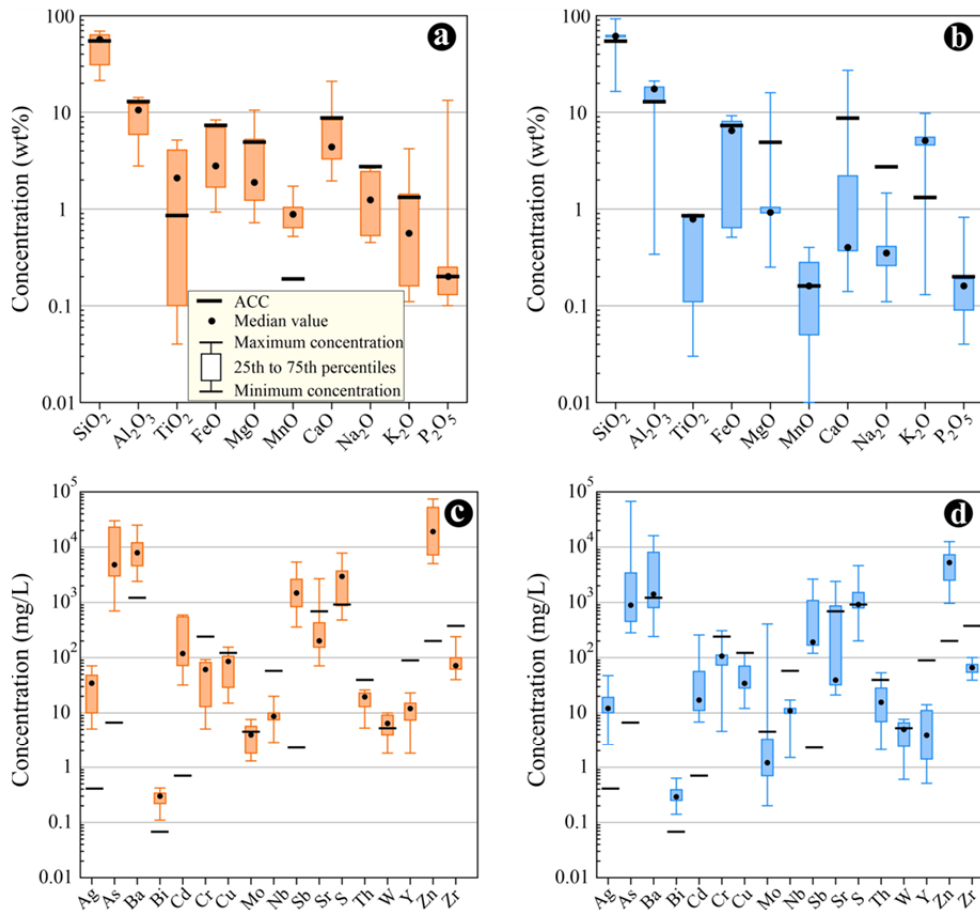


**Figure 4** Boxplots presenting summary statistics for selected whole rock major (wt%) and trace element concentration (mg/L) on ore-bearing and host rock samples. (a) Ore-bearing and (b) host rocks of major element. (c) Ore-bearing and (d) host rocks of trace element. ACC: Average composition of continental crust (Yaroshevsky 2006).

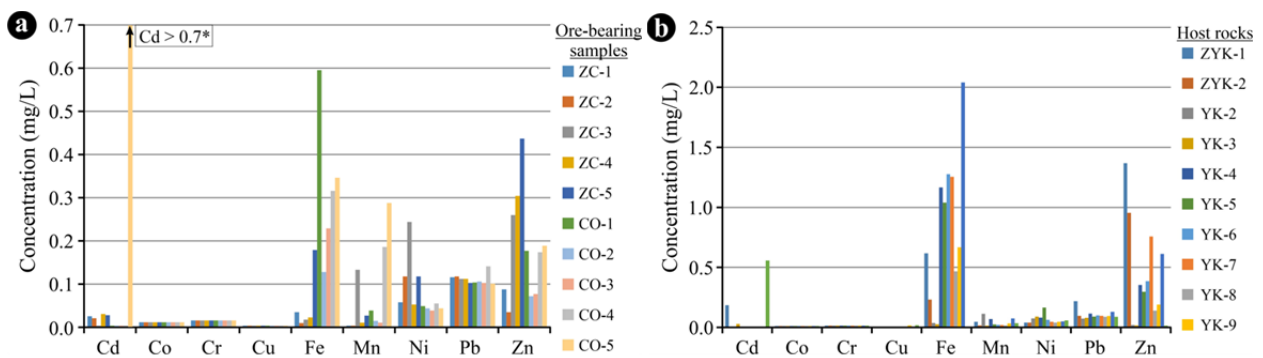


**Figure 5** Selected potentially toxic metal concentrations of filtered and/or acidified water of the (a) ore-bearing samples and (b) host rocks. \*The Cd value of this sample is 3.58 mg/L.

**Table 3** Results of contact leaching tests (mg/L) of the ore-bearing samples and host rocks from mineralization area

	pH	Na	Al	Cd	Co	Cr	Cu	Fe	Mn	Ni	Pb	Zn
Quality Classification of the Intra-Continental Water Resources*												
I	6.5-8.5	125	≤0.3	≤0.002	≤0.01	≤0.02	≤0.02	≤0.3	≤0.1	≤0.02	≤0.01	≤0.2
II	6.5-8.5	125	≤0.3	0.005	0.02	0.05	0.05	1	0.5	0.05	0.02	0.5
III	6.0-9.0	250	1	0.007	0.2	0.2	0.2	5	3	0.2	0.05	2
IV	<6.0/>9.0	>250	>1	>0.007	>0.2	>0.2	>0.2	>5	>3	>0.2	>0.05	>2
Sample	Host rocks (limestone, dolomite, quartzite and schist)											
ZYK-1	7.68	10.16	5.09	0.185	<0.01	<0.02	<0.02	0.62	0.05	0.04	0.22	1.37
ZYK-2	7.92	6.64	0.76	<0.002	<0.01	<0.02	<0.02	0.23	0.02	0.04	0.10	0.96
YK-2	8.56	2.50	0.03	<0.002	<0.01	<0.02	<0.02	0.04	0.11	0.08	0.07	0.02
YK-3	9.00	5.91	0.02	0.028	<0.01	<0.02	<0.02	0.03	0.02	0.09	0.08	0.02
YK-4	8.09	3.63	1.68	<0.002	<0.01	<0.02	<0.02	1.17	0.07	0.08	0.12	0.35
YK-5	7.86	5.23	1.18	<0.002	<0.01	<0.02	<0.02	1.04	0.03	0.17	0.09	0.30
YK-6	7.86	3.08	1.49	<0.002	<0.01	<0.02	<0.02	1.28	0.02	0.06	0.10	0.39
YK-7	7.65	3.05	1.52	<0.002	<0.01	<0.02	<0.02	1.26	0.02	0.05	0.10	0.76
YK-8	8.00	4.22	0.91	<0.002	<0.01	<0.02	<0.02	0.47	0.02	0.04	0.09	0.14
YK-9	8.29	6.03	1.01	<0.002	<0.01	<0.02	0.02	0.67	0.03	0.05	0.10	0.19
YK-10	7.95	3.94	2.64	<0.002	<0.01	<0.02	<0.02	2.04	0.08	0.05	0.13	0.61
YK-10A	8.32	1.66	0.08	0.558	<0.01	<0.02	0.02	<0.01	0.04	0.06	0.09	0.02
Sample	Ore-bearing samples											
ZC-1	8.24	4.64	0.04	0.026	<0.01	<0.02	<0.02	0.04	<0.01	0.06	0.12	0.09
ZC-2	8.47	6.44	≤0.3	0.021	<0.01	<0.02	<0.02	0.01	<0.01	0.12	0.12	0.04
ZC-3	8.11	8.25	≤0.3	<0.002	<0.01	<0.02	<0.02	0.02	0.13	0.24	0.11	0.26
ZC-4	7.94	9.85	≤0.3	0.031	<0.01	<0.02	<0.02	0.02	0.01	0.05	0.11	0.30
ZC-5	8.19	5.67	0.13	0.028	<0.01	<0.02	<0.02	0.18	0.03	0.12	0.10	0.44
CO-1	8.20	6.25	0.91	<0.002	<0.01	<0.02	<0.02	0.60	0.04	0.05	0.10	0.18
CO-2	8.27	4.58	0.27	<0.002	<0.01	<0.02	<0.02	0.13	0.02	0.04	0.11	0.07
CO-3	8.33	6.79	0.46	<0.002	<0.01	<0.02	<0.02	0.23	0.01	0.04	0.10	0.08
CO-4	8.16	4.03	0.65	<0.002	<0.01	<0.02	<0.02	0.32	0.19	0.06	0.14	0.17
CO-5	7.98	6.64	0.81	3.582	<0.01	<0.02	<0.02	0.35	0.29	0.04	0.10	0.19

**Note:** \*RG28483 (2012): Regulation on Surface Water Quality Management, the Turkish Standards, 30.11.2012, number 28483 (revision: RG-15.4.2015-29327).

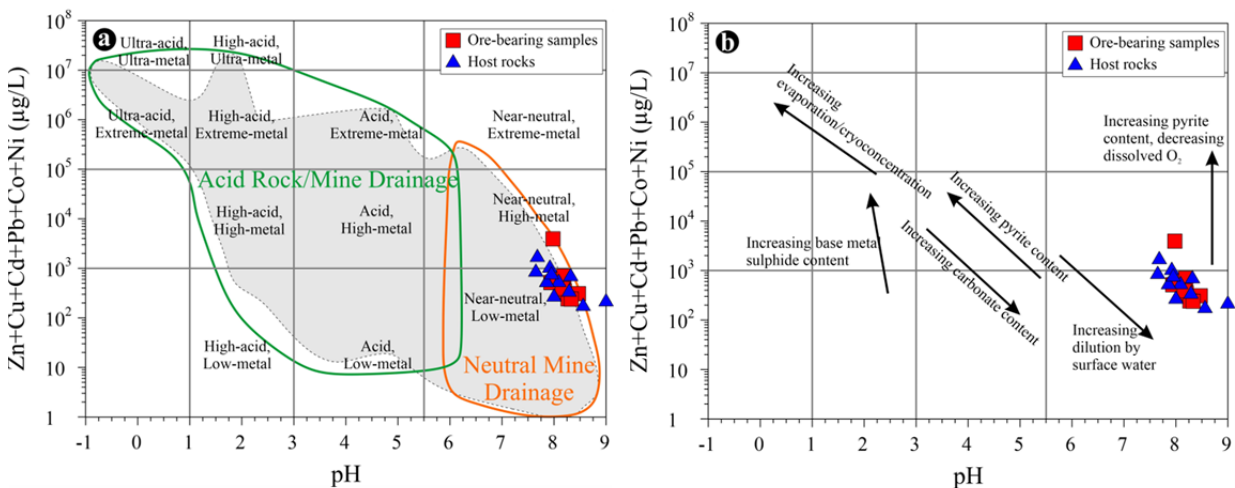


**Figure 6** (a) Ficklin geochemical discrimination diagram for the samples. (b) Trending of the samples in the Ficklin classification plot (grey area adapted from Plumlee et al. 1999).

dilution and reduced solid to water ratio, associated with wetter climates and geological setting (e.g., limestone/ dolomite rocks, mica schists, etc.) of the study area.

### 3.3 Assessment of acid-base accounting

The ABA is defined simply as the balance between the acid-production and acid-consumption properties of mine waste material (e.g., Smith et al. 1976; Skousen et al. 1987). It is used to make static measurements of acid mine drainage potential. Measurements of total sulphur (S%) and sulphide sulphur (S<sup>2-</sup>) are used to

estimate the amount of acid-bearing material. ABA static measurement results in the mine and stockpile areas are provided in Table 4. The interpretation of the ABA formation is based on some criteria as shown in Table 5.

In the study area, paste pH values of the ore-bearing samples ranged between 7.39-8.34, whereas host rocks varied from 7.36 to 9.38. This indicated that the rocks in the study area are non-acid producing according to Table 5. Also, if the materials have less than 0.3% sulphide-sulphur concentrations, acid producing does not occur because of not contain enough sulphide to sustain acid generating chemical reactions (e.g. Sobek et al. 1978). Therefore, acid producing materials have a sulphide-sulphur concentration greater than 0.3%, and they have neutralization potential ratio (NPR) less than 3:1 ratio. In case of a sulphide-sulphur concentration between 0.1% and 0.3%, the materials have a low probability of being potentially acid generating in the field (Figure 7). The NNP contents of the ore-bearing rocks ranged in between 18.7-439 kg/t CaCO<sub>3</sub> and samples plot predominantly in the non-acid producing field (Figure 8a). However, host rocks contain NNP ranged from 1.72-716 kg/t CaCO<sub>3</sub> (n=12) and cluster mostly in uncertainty area (Figure 8a). In all samples, the NPR (NP/AP) values varied between 3.53 and 1155 (n= 21) and scattered in the non-acid producing area (Figure 8b).

### 3.4 Investigation of the permeability of stock area rock mass

To determine the hydraulic conductivity value of the rock mass that forms the basis of the stock area, pumping tests were performed in the drilled well and the aquifer characteristics were determined using these experimental results. Hydraulic conductivity was determined by three different methods (Jacob’s graphic method, Theis method, and Neuman method) and the average of the obtained values was used in the numerical analysis method.

The average hydraulic conductivity (permeability) value of the rock mass obtained from the pumping tests is  $K= 1.9 \times 10^{-6}$  m/s, and it is moderately permeable according to the classification proposed by Bell (1992) (Table 6). In this case, the ore storage that will be done without taking any precautions in the stock area will pollute

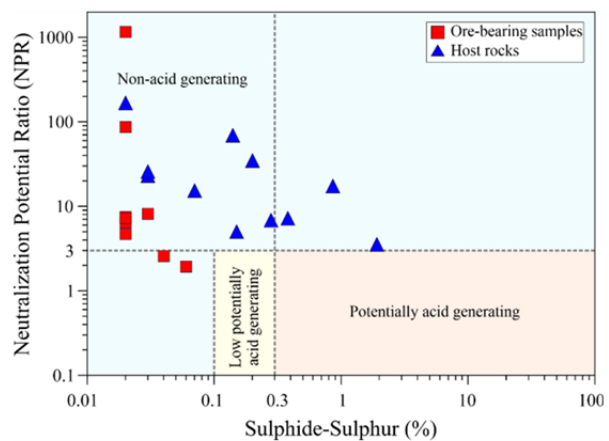


**Figure 7** Neutralization Potential Ratio (NPR) vs Sulphide-Sulphur (%) diagram showing acid prediction zones and distribution of studied samples.

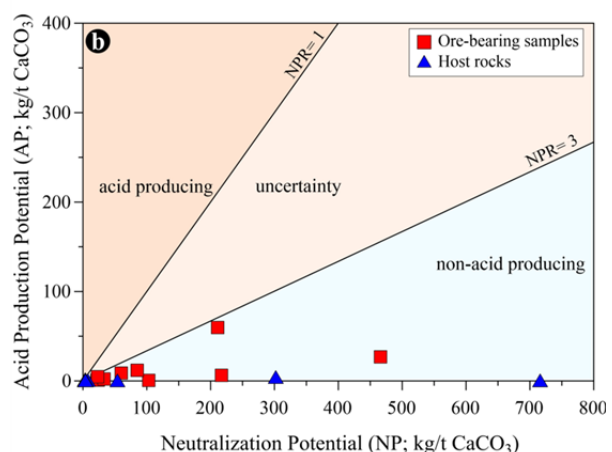
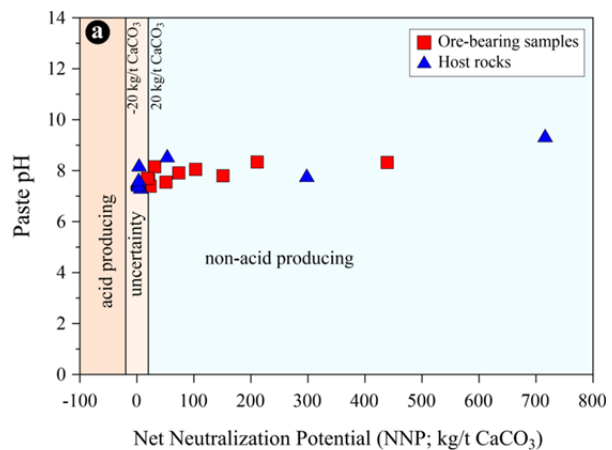


**Figure 8** The acid-base accounting (ABA) diagrams of studied rocks. (a) Paste pH versus net neutralization potential (NNP) and, (b) acid production potential (AP) versus neutralization potential (NP) of carbonate.

the water that will accumulate in the crack system of the rock mass. To prevent this situation, natural clay will be laid and compacted on the floor of the

**Table 4** Acid Base Accounting (ABA) analyses of the ore-bearing samples and host rocks from mineralization area

Sample	Paste pH	NP	AP	NNP	Sulphur Total S	Acid leachable sulfate (SO <sub>4</sub> <sup>2-</sup> )	Sulphide S <sup>2-</sup>	Carbon (total C)	Carbonate CaCO <sub>3</sub>
Unit	–	kg/t CaCO <sub>3</sub>	kg/t CaCO <sub>3</sub>	kg/t CaCO <sub>3</sub>	%	%	%	%	%
Sample	Host rocks (limestone, dolomite, quartzite and schist)								
ZYK-1	7.52	3.2	1.25	1.95	0.074	0.03	0.04	0.022	0.055
ZYK-2	7.36	7.6	0.94	6.66	0.03	<0.02	0.03	0.033	0.125
YK-2	8.59	54	0.62	53.3	0.029	<0.02	0.02	0.718	3.17
YK-3	9.38	716	0.62	716	0.036	0.04	<0.02	9.76	41.3
YK-4	7.60	3.6	1.88	1.72	0.074	<0.02	0.06	0.048	0.085
YK-5	7.56	4.6	0.62	3.98	<0.005	<0.02	<0.02	0.063	0.105
YK-6	7.60	4	0.62	3.38	0.011	<0.02	<0.02	0.1	0.115
YK-7	7.49	2.9	0.62	2.28	0.011	<0.02	<0.02	0.039	0.05
YK-8	8.23	4.5	0.62	3.88	0.015	<0.02	<0.02	0.036	0.05
YK-9	7.44	3.7	0.62	3.08	<0.005	<0.02	<0.02	0.049	0.08
YK-10	7.66	3.9	0.62	3.28	<0.005	<0.02	<0.02	0.035	0.055
YK-10A	7.82	302	4.38	298	0.176	0.04	0.14	3.82	17.5
Sample	Ore-bearing samples								
ZC-1	7.80	211	59.7	151	1.9	<0.02	1.91	3.04	12.2
ZC-2	8.32	466	26.9	439	0.972	0.11	0.86	5.44	27.5
ZC-3	7.62	22	0.94	20.7	0.077	0.05	0.03	0.177	0.465
ZC-4	8.05	103	0.62	103	0.25	0.25	<0.02	1.09	4.88
ZC-5	7.39	24	0.94	23.2	0.043	<0.02	0.03	0.233	0.709
CO-1	8.15	33	2.19	31.2	0.083	<0.02	0.07	0.5	1.86
CO-2	7.55	60	8.75	51	0.353	0.07	0.28	0.746	2.8
CO-3	8.34	217	6.25	211	0.282	0.08	0.2	2.51	11.6
CO-4	7.70	23	4.69	18.7	0.22	0.07	0.15	0.252	0.764
CO-5	7.91	85	11.9	73.5	0.435	0.06	0.38	1.05	4.19

**Note:** NP: Neutralization potential. AP: Acid production potential. NNP: Net neutralization potential (NNP= NP – AP). Samples with a % Sulphide value of <0.02 will be calculated using a 0.02 value.

**Table 5** Static test interpretation parameters.

References	Screening criterion		Paste pH
	NPR	NNP	
Price et al. (1997)	<1, Likely AMD potential		pH<4, Acid pH>7, Neutral
	1-2, Possibly AMD potential		
	2-4, Low AMD potential		
	>4, None		
Soregaroli and Lawrence (1998)	<1, Potential acid formation		
	1-3, Inconclusive		
	>4, Has enough neutralizing capacity		
Brodie et al. (1991)	<1, Acid generating		
	1-3, Uncertain		
	>3, None acid generating		
Ferguson and Morin (1991)		<-20, Potential acid formation	
		-20<NNP<20, Uncertain	
		>20, Non-acid formation	
Sobek et al. (1978)		<-5, Acid forming	

**Note:** The unit of measurement is kg CaCO<sub>3</sub> per ton, or equivalently parts per thousand CaCO<sub>3</sub>. NNP: Net neutralization potential. NPR: Neutralization potential ratio.

stock area. The properties of the clay to be laid on the stock field were determined and the soil class CL (low plasticity clay), maximum dry unit weight of the compressed clay material in proctor energy

was 15.99 kN/m<sup>3</sup> and the permeability value obtained in the falling head permeability test of the compressed material was 5.23×10<sup>-10</sup> m/s. The clay, which is planned to be laid on the base of the stock

**Table 6** Aquifer characteristics and permeability classification.

Analysis method	<i>T</i>	<i>K</i>	Permeability	Permeability degree (m/s) (Bell 1992)
Jacob Graphic Method	10	$2.3 \times 10^{-6}$	Highly permeable	$10^{-2}$ -1
Theis Method	7.5	$1.7 \times 10^{-6}$	Moderately permeable	$10^{-5}$ - $10^{-2}$
Neuman Method	7.5	$1.7 \times 10^{-6}$	Slightly permeable	$10^{-9}$ - $10^{-5}$
Arithmetic Mean	8.3	$1.9 \times 10^{-6}$	Impermeable	$<10^{-9}$

**Note:** *T*: Transmissibility (m<sup>2</sup>/day). *K*: Hydraulic Conductivity (m/s).

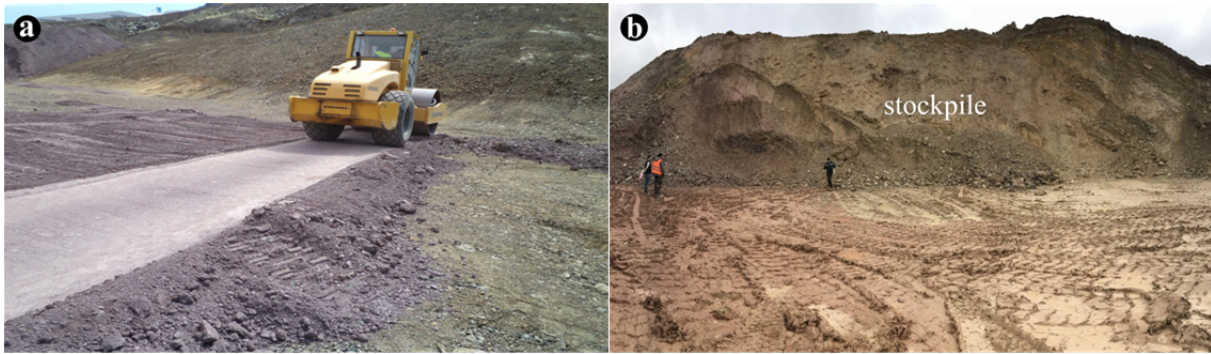


**Figure 9** (a) Application example for laying and compressing clay in the stock field. (b) Ore deposit and stock field in the study area.

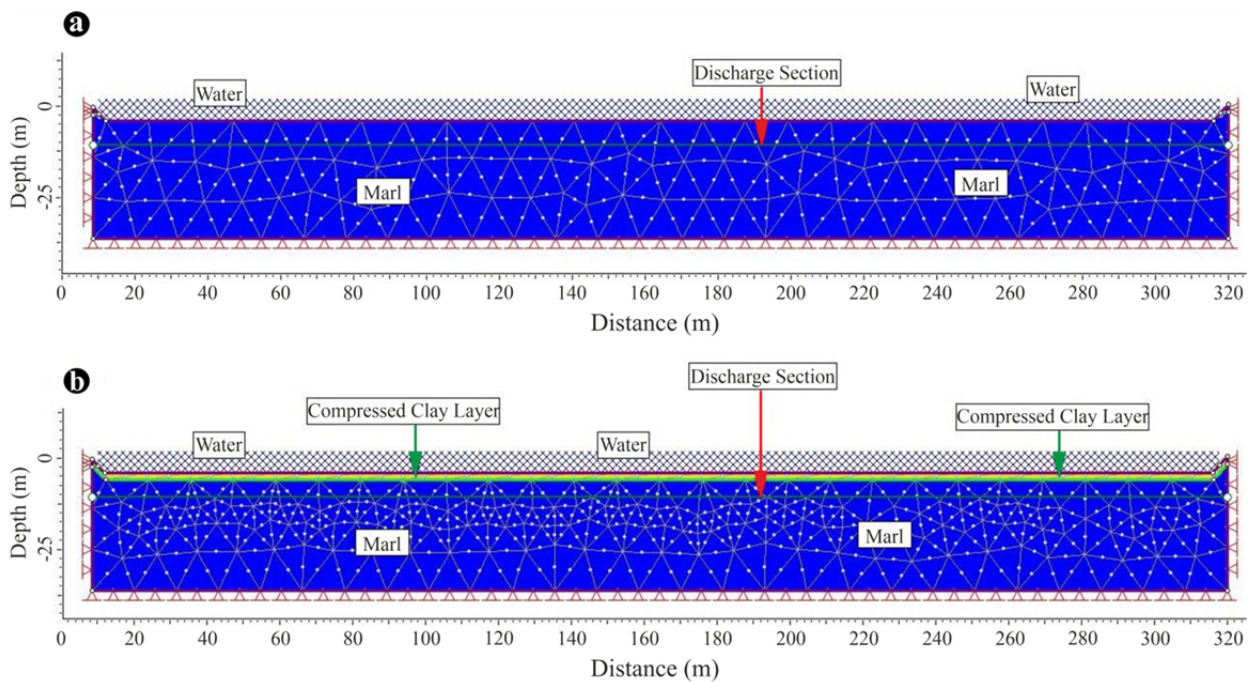


**Figure 10** Finite element network model used in numerical analysis. a) The model before improvement in stockpile. b) The model after compacting clay on the stockpile floor.

area and to be compressed by roller, should be 30 cm thick (Figure 9). Thus, it is expected to stop AMD leaking into the groundwater, which is expected to occur in the future. The marl at the base of the stock area were moderately permeable and after the improvement application, the base

stock area rock mass was modeled by using the finite element method in RS2 (Rocscience 2019) software. Impermeability and seepage discharges of the environment were determined by two-dimensional finite element seepage analysis.

Modeling of the bedrock of the stock area

**Table 7** The parameters used in numerical analysis.

Material Properties	Marl	Material Properties	Compressed Clay
Unit weight (MN/m <sup>3</sup> )	0.02069	Unit weight	0.01599
Elastic type	isotropic	Elastic type	isotropic
Young's modulus (MPa)	80.9	Young's modulus	4
Poisson's ratio	0.36	Poisson's ratio	0.4
Failure Criterion	Generalized Hoek-Brown	Failure Criterion	Mohr-Coulomb
Material type	Plastic	Peak friction angle	12°
Compressive strength (MPa)	3.37	Peak Cohesion (MPa)	0.1
<i>m<sub>b</sub></i>	0.3057	Residual Friction Angle	7°
<i>s</i>	0.00033	Residual Cohesion (MPa)	0.04
<i>a</i>	0.5256	<i>K</i> (m/s)	5.23e-010
Hydraulic model	Simple	<i>K<sub>2</sub>/K<sub>1</sub></i>	1
<i>K</i> (m/s)	1.9e-06		
<i>K<sub>2</sub>/K<sub>1</sub></i>	1		

**Note:** *m<sub>b</sub>*, *s*, *a*: Hoek-Brown Constants. *K*: Hydraulic Conductivity (m/s). *K<sub>2</sub>/K<sub>1</sub>*: The relative permeability in the direction orthogonal to the *K<sub>1</sub>* direction.

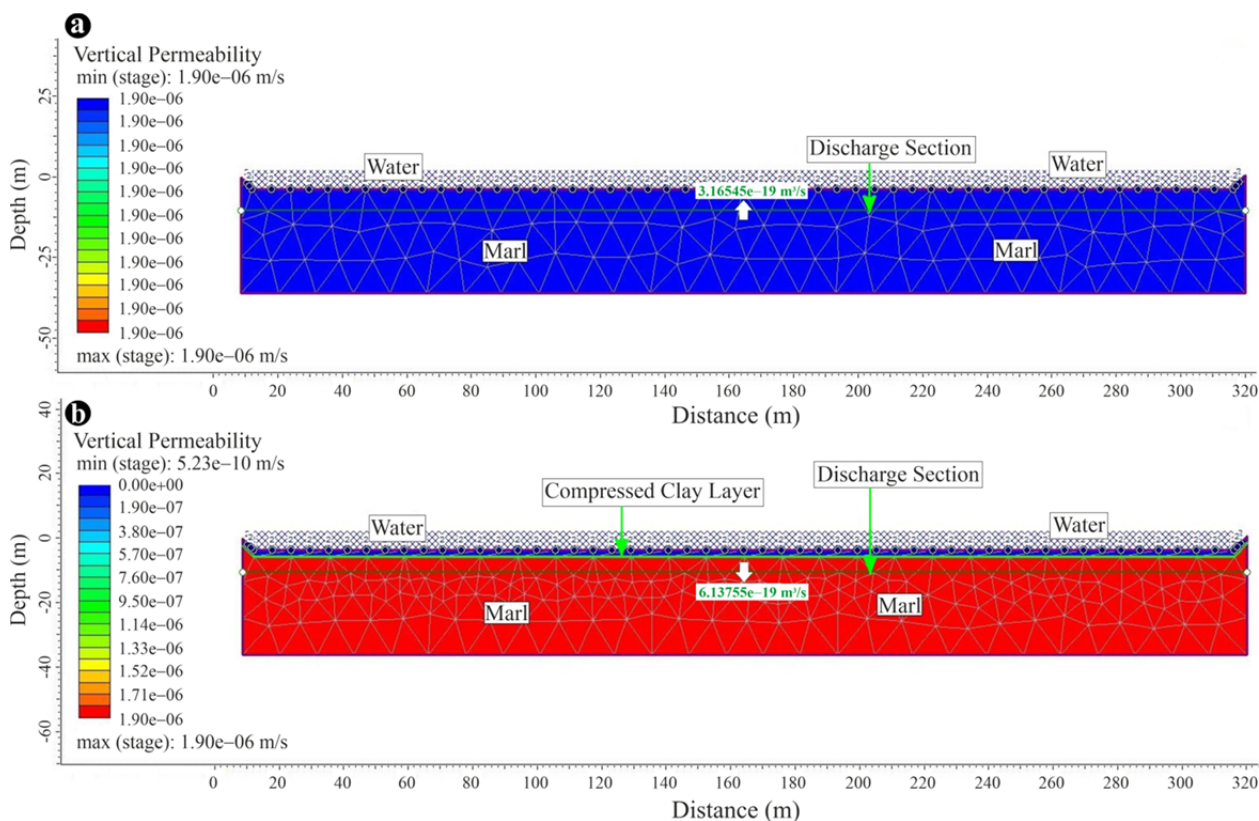


**Figure 11** The vertical permeability analysis in the stock area. a) The model before improvement in stockpile. b) The model after compacting clay on the stockpile floor.

before and after the improvement with the finite element network system is given in Figure 10 and the parameters used in the analysis are given in Table 7.

According to the finite element method network model (Figure 11a), it was determined that the hydraulic conductivity value of the bedrock of the stock area was  $K = 1.9 \times 10^{-6}$  m/s, and the seepage discharge value at the depth of 5 m from

the surface was  $3.17 \times 10^{-19}$  m<sup>3</sup>/s. After the clay compression to be applied to the base of the stock area (Figure 11b), the rock mass permeability value was determined to vary between  $1.9 \times 10^{-6}$  m/s and  $5.23 \times 10^{-10}$  m/s and the leakage discharge value was  $6.14 \times 10^{-19}$  m<sup>3</sup>/s at the same depth. These results indicate that the rock mass is theoretically impermeable after the improvement.

#### 4 Conclusions and Suggestions

The results of the studies to determine the formation of mine drainage in the ore deposit and stock areas and, the prevention studies in case of a possible mine drainage development are summarized below.

- The whole rock major element content of both host rocks and ore-bearing samples have close to or below the average composition of the continental crust depending on the mineralogical composition of the rocks. Similarly, the trace element distributions of all samples display a higher enrichment compared to the average continental crust composition in relation to mineralization and hydrothermal alteration. The high enrichment in some heavy metals such as Ag, Cd, Mo, Ba, Bi, and Zn is also directly related to mineralization.

- The obtained pH values in all samples indicate alkaline environment rather than the acidic, and the data shows class-I water quality characteristics according to the classification of intra-continental water resources. Besides, the studied rocks have neutral mine drainage characteristics in reference to base metal concentrations.

- According to the ABA tests, paste pH and very low  $S^{2-}$  data, acid mine drainage formation has not been expected in the mineralization area. In addition, this is supported by the NNP ( $>20$  kg/t  $CaCO_3$ ) and NPR ( $>3$ ) values.

- When static tests are evaluated on the ore material to be poured into the stock area, the potential for mine drainage formation in the mineralization area is not expected in a short time. However, in order to prevent possible formation of mine drainage in the long-term, 30cm clay should be laid and compacted on the base of the stock area.

- The hydraulic conductivity value of the

marl rock mass, which constitutes the basement rock of the stock field, was determined as  $K=1.9 \times 10^{-6}$  m/s as a result of the pumping tests performed in situ. When the value was evaluated according to the permeability classification, it was determined that the rock mass in the stock area was moderately permeable in the vertically distribution.

- The clay compaction process to be applied at the stock area base was modeled by seepage analysis using the finite element method, and the minimum permeability value of the rock mass after improvement was determined as  $5.23 \times 10^{-10}$  m/s. In the same model, the seepage discharge at the depth of 5m from the surface of the rock mass was determined as  $3.17 \times 10^{-19}$  m<sup>3</sup>/s. The bedrock would completely be impermeable after the ground improvement and the groundwater contamination from the possible mine drainage formation would be prevented. In addition, in order to prevent possible seepage in the stockpile, it should be surrounded by drainage channel the stock area, and mine drainage remediation should be ensured by laying limestone on the channel.

- Additionally, sulfate-reducing bioreactor or steel slag bed may have more efficiency to remove Zn.

#### Acknowledgments

We would like to thank the company of Eti Gümüş AŞ, which provided financial support to this study and helped to collect and analyze samples from the study area. Special thanks also go to staff members at the company of Eti Gümüş AŞ, especially Mahir ATLI, for their support and assistance with this study. We would also like to thank the editors and reviewers for their constructive and article developer suggestions.

#### References

- Akaryalı E, Gücer MA, Alemdag S (2018) Assessment of acid mining drainage (AMD) formation in the ore stock and waste dam reservoir areas: An example of Gümüşhane. *Journal of Natural Hazards and Environment* 4(2): 192-209. <https://doi.org/10.21324/dacd.415259>
- Akçıl A, Koldaş S (2006) Acid Mine Drainage (AMD): Causes, treatment and case studies. *Journal of Cleaner Production*

- 14(12-13): 1139-1145. <https://doi.org/10.1016/j.jclepro.2004.09.006>
- Aldanmaz E, Yalınız MK, Güçtekin A, et al. (2008) Geochemical characteristics of mafic lavas from the Tethyan ophiolites in western Turkey: implications for heterogeneous source contribution during variable stages of ocean crust generation. *Geological Magazine* 145: 37-54.

- <https://doi.org/10.1017/S0016756807003986>  
 Alemdag S (2015) Assessment of bearing capacity and permeability of foundation rocks at the Gumustas waste dam site, (NE Turkey) using empirical and numerical analysis. *Arabian Journal of Geosciences* 8: 1099-1110.  
<https://doi.org/10.1007/s12517-013-1236-3>
- Alemdağ S, Akaryalı E, Gücer MA (2020) Acid Production Potential of Flotation Plant Tailings and Pollution Prevention, Gumushane, Turkey NE. *Bulletin for Earth Sciences* 41(1): 56-85.  
<https://doi.org/10.17824/yerbilimleri.693508>
- Arik F (2002). Geochemical modelling of Gümüşköy (Kütahya) silver deposit. PhD Dissertation, Institute of the Natural and Applied Sciences, Selçuk University. (In Turkish)
- Arik F (2008). Geological, petrographical and geochemical characteristics of Sığireğreği (Şahin-Kütahya) Zn-Pb ore deposit. Symposium on geology, mining and present problems of lead-zinc deposits of Türkiye. Istanbul University, Department of Geological and Mining Engineering, pp 154-183.
- Arik F (2012). Genetic characteristics of the Gözeçukuru As-Sb deposits near Kütahya, Turkey. *Journal of the Geological Society of India* 80: 855-868.  
<https://doi.org/10.1007/s12594-012-0214-9>
- Arik F, Yaldız T (2010). Heavy metal determination and pollution of the soil and plants of southeast Tavşanlı (Kütahya, Turkey). *CLEAN-Soil Air Water* 38(11): 1017-1030.  
<https://doi.org/10.1002/clen.201000131>
- ASTM E1915-07A (2007). Standard Test Methods for Analysis of Metal Bearing Ores and Related Materials by Combustion Infrared-Absorption Spectrometry, ASTM International, West Conshohocken, PA, USA.
- Bell F G (1992). *Engineering in Rock Masses*, Butterworth-Heinemann, Oxford, p 580.
- Berghorn GH, Hunzeker GR (2001). Passive treatment alternatives for remediating abandoned-mine drainage. *Remediation* 11: 111-127.  
<https://doi.org/10.1002/rem.1007>
- Betfie GD, Sadiq R, Morin KA, et al. (2015). Ecological risk assessment of acid rock drainage under uncertainty: The fugacity approach. *Environmental Technology and Innovation* 4: 240-247.  
<https://doi.org/10.1016/j.eti.2015.07.004>
- Boon M, Heijnen JJ (1998). Chemical oxidation kinetics of pyrite in bioleaching processes. *Hydrometallurgy* 48: 27-41.  
[https://doi.org/10.1016/S0304-386X\(97\)00072-8](https://doi.org/10.1016/S0304-386X(97)00072-8)
- Bouffard SC, Rivera-Vasquez BF, Dixon DG (2006). Leaching kinetics and stoichiometry of pyrite oxidation from a pyrite-marcasite concentrate in acid ferric sulfate media. *Hydrometallurgy* 84: 225-238.  
<https://doi.org/10.1016/j.hydromet.2006.05.008>
- Brodie MJ, Broughton LM, Robertson A (1991). A conceptual rock classification system for waste management and a laboratory method for ARD prediction from rock piles. 2nd International Conference on Acid Rock Drainage (ICARD) proceedings 3: 119-135.
- Brunner B, Yu J-Y, Mielke RE, et al. (2008). Different isotope and chemical patterns of pyrite oxidation related to lag and exponential growth phases of *Acidithiobacillus ferrooxidans* reveal a microbial growth strategy. *Earth and Planetary Science Letters* 270: 63-72.  
<https://doi.org/10.1016/j.epsl.2008.03.019>
- Caraballo MA, Rötting TS, Macias F, et al. (2009). Field multi-step limestone and MgO passive system to treat acid mine drainage with high metal concentrations. *Applied Geochemistry* 24: 2301-2311.  
<https://doi.org/10.1016/j.apgeochem.2009.09.007>
- Çimen O (2019). Geochemical characteristics of a pre-Middle Jurassic oceanic crust fragment from the Central Pontides in northern Turkey: Geodynamic implications on intra-oceanic subduction initiation. *Geochemistry* 80(1): 125535.  
<https://doi.org/10.1016/j.chemer.2019.125535>
- Çimen O, Öztüfekçi-Önal A (2018) Preliminary geochemical data of the mafic rocks from the Ovacik and Pülümür Ophiolite Zone (Eastern Anatolia, Turkey): Implications for the geodynamic evolution of the northern Neotethyan Ocean. *Ofioliti* 43(2): 103-116.  
<https://doi.org/10.4454/ofioliti.v43i2.458>
- Çimen O, Göncüoğlu MC, Sayit K (2016). Geochemistry of the metavolcanic rocks from the Çangaldağ Complex in the Central Pontides: implications for the Middle Jurassic arc-back-arc system in the Neotethyan Intra-Pontide Ocean. *Turkish Journal of Earth Sciences* 25: 491-512.  
<https://doi.org/10.3906/yer-1603-11>
- Çimen O, Göncüoğlu MC, Simonetti A, et al. (2017). Whole rock geochemistry, Zircon U-Pb and Hf isotope systematics of the Çangaldağ Pluton: Evidences for Middle Jurassic Continental Arc Magmatism in the Central Pontides, Turkey. *Lithos* 290-291: 136-155.  
<https://doi.org/10.1016/j.lithos.2017.06.020>
- Çimen O, Göncüoğlu MC, Simonetti A, et al. (2018). New zircon U-Pb LA-ICP-MS ages and Hf isotope data from the Central Pontides (Turkey): Geological and geodynamic constraints. *Journal of Geodynamics* 116: 23-36.  
<https://doi.org/10.1016/j.jog.2018.01.004>
- Delibalta MS, Uzal N, Lermi A (2016). Acid mine drainage and rehabilitation in Iğın Lignite Mines Lakes. *Nigde University Journal of Engineering Sciences* 5(1): 73-82.  
<https://doi.org/10.28948/ngumuh.239350>
- Descostes M, Vitorge P, Beaucaire C (2004). Pyrite dissolution in acidic media. *Geochimica et Cosmochimica Acta* 68: 4559-4569.  
<https://doi.org/10.1016/j.gca.2004.04.012>
- EPA (US Environmental Protection Agency) (1983). *Neutralization of Acid Mine Drainage*, Cincinnati, USA.
- EPA (US Environmental Protection Agency) (1994a). *Innovative Methods of Managing Environmental Releases at Mine Sites*, USEPA, Office of Solid Waste, Special Wastes Branch (Washington DC), April, OSW Doc. 530-R-94-012.
- EPA (US Environmental Protection Agency) (1994b). *Acid Mine Drainage Prediction*, USEPA, Office of Solid Waste, Special Wastes Branch (Washington DC), December, EPA 530-R-94-036.
- Ferguson KD, Morin KA (1991). The prediction of acid rock drainage - lessons from the database. In: *Proceedings of the 2nd ICARD*, 1-4: Montréal, QC, Canada, pp 83-106.
- Frostad SR, Price WA, Bent H (2003). Operational NP determination-accounting for iron manganese carbonates and developing a site-specific fizz rating. In: Spiers G, Beckett P, Conroy H (eds), *Mining and the environment*. Laurentian University, Sudbury, pp 231-237.
- Gleisner M, Herbert RB, Kockum PCF (2006). Pyrite oxidation by *Acidithiobacillus ferrooxidans* at various concentrations of dissolved oxygen. *Chemical Geology* 225: 16-29.  
<https://doi.org/10.1016/j.chemgeo.2005.07.020>
- Gücer MA, Arslan M, Çimen O, et al. (2019) Petrology and <sup>40</sup>Ar-<sup>39</sup>Ar dating of paragneisses from the Devrekani Massif (Central Pontides, Northern Turkey): Implications for the Jurassic high-T metamorphism in an extensional tectonic environment. *Journal of Asian Earth Sciences* 181: 103888.  
<https://doi.org/10.1016/j.jseae.2019.103888>
- Gücer MA, Arslan M, Sherlock SC, et al. (2016). Permo-Carboniferous granitoids with Jurassic high temperature metamorphism in Central Pontides, Northern Turkey. *Mineralogy and Petrology* 110(6): 943-964.  
<https://doi.org/10.1007/s00710-016-0443-5>
- Gurocak Z, Alemdag S (2012). Assessment of permeability and injection depth at the Atasu dam site (Turkey) based on experimental and numerical analyses. *Bulletin of Engineering Geology and the Environment* 71: 221-229.  
<https://doi.org/10.1007/s10064-011-0400-9>
- Hoek E, Carranza-Torres CT, Corkum B (2002) Hoek-Brown failure criterion-2002 edition. In: *Proceedings of the 5<sup>th</sup> North American Rock Mechanics Symposium*; Toronto, Canada. pp.



- 267-273.
- Holmes PR, Crundwell FK (2000). The kinetics of the oxidation of pyrite by ferric ions and dissolved oxygen: an electrochemical study. *Geochimica et Cosmochimica Acta* 64: 263-274.  
[https://doi.org/10.1016/S0016-7037\(99\)00296-3](https://doi.org/10.1016/S0016-7037(99)00296-3)
- ISRM (International Society for Rock Mechanics) (2007) The complete ISRM suggested methods for rock characterization. In: Ulusay R, Kazan Hudson JA (eds). *Testing and Monitoring*. Offset Press, Ankara. p.628.
- Jia Y, Tan Q, Sun H, et al. (2018). Sulfide mineral dissolution microbes: Community structure and function in industrial bioleaching heaps. *Green Energy and Environment* 4(1): 29-37.  
<https://doi.org/10.1016/j.gee.2018.04.001>
- Kalyoncu Erguler G, Erguler ZA (2020). The evaluation of acid mine drainage by kinetic procedures and empirical models for field scale behaviour. *Arabian Journal of Geosciences* 13: 387.  
<https://doi.org/10.1007/s12517-020-05372-0>
- Kank M, Ersoy H (2019). Evaluation of the engineering geological investigation of the Ayvalı dam site (NE Turkey). *Arabian Journal of Geosciences* 12: 89.  
<https://doi.org/10.1007/s12517-019-4243-1>
- Kim DM, Yun ST, Cho Y, et al. (2017). Hydrochemical assessment of environmental status of surface and groundwater in mine areas in South Korea: Emphasis on geochemical behaviors of metals and sulfate in ground water. *Journal of Geochemical Exploration* 183: 33-45.  
<https://dx.doi.org/10.1016/j.gexplo.2017.09.014>
- Lawrence RW, Scheske M (1997) A method to calculate the neutralization potential of mining wastes. *Environmental Geology* 32: 100-106.  
<https://doi.org/10.1007/s002540050198>
- Lawrence RW, Wang Y (1996) Determination of neutralizing potential for acid rock drainage prediction. MEND/NEDEM report 1.16.3, Canadian Centre for Mineral and Energy Technology, Ottawa, ON, Canada.
- Lefebvre C, Meijers MJM, Kaymakçı N, et al. (2013). Reconstructing the geometry of central Anatolia during the late Cretaceous: large-scale Cenozoic rotations and deformation between the Pontides and Taurides. *Earth and Planetary Science Letters* 366: 83-98.  
<https://doi.org/10.1016/j.epsl.2013.01.003>
- Liu C, Jia Y, Sun H, et al. (2017) Limited role of sessile acidophiles in pyrite oxidation below redox potential of 650 mV. *Scientific Reports* 7(1): 5032.  
<https://doi.org/10.1038/s41598-017-04420-2>
- Lottermoser BG, Ashley PM (2011) Trace element uptake by *Eleocharis equisetina* (spike rush) in an abandoned acid mine tailings pond, northeastern Australia: Implications for land and water reclamation in tropical regions. *Environmental Pollution* 159: 3028-3035.  
<https://doi.org/10.1016/j.envpol.2011.04.014>
- Ma Y, Lin C (2013) Microbial oxidation of Fe and pyrite exposed to flux of micromolar H<sub>2</sub>O<sub>2</sub> in acidic media. *Scientific Reports* 3: 1350-1352.  
<https://doi.org/10.1038/srep01979>
- Marchand L, Mench M, Jacob DL, et al. (2010). Metal and metalloid removal in constructed wetlands, with emphasis on the importance of plants and standardized measurements: a review. *Environmental Pollution* 158: 3447-3461.  
<https://doi.org/10.1016/j.envpol.2010.08.018>
- Meijers MJM, Langereis CG, van Hinsbergen DJJ, et al. (2010). Jurassic-Cretaceous low paleolatitudes from the circum-Black Sea region (Crimea and Pontides) due to True Polar Wander. *Earth and Planetary Science Letters* 296: 210-226.  
<https://doi.org/10.1016/j.epsl.2010.04.052>
- MEND (Mine Environment Neutral Drainage) (2009). Prediction manual for drainage chemistry from sulphidic geologic materials. In: CANMET-Mining and Mineral Sciences Laboratories, Smithers, British Columbia, Canada. MEND report 1.20.1, 579 p.
- Miller SD, Jeffery JJ, Wong JWC (1991). Use and misuse of the acid base account for "AMD" prediction. In: *Proceedings of the 2nd ICARD*, vol-3. Montreal, QC, Canada, pp 489-506.
- Mills C (1995). An AMD/ARD dedicated blog based on the text of a presentation given Mills to British Columbia High School Science Teachers. Seminar; Acid Rock Drainage at the Cordilleran Roundup, Hotel Vancouver, Vancouver, BC.
- Morin KA, Hutt NM (2001). *Environmental geochemistry of minesite drainage: practical theory and case studies*. MDAG Publishing, Vancouver.
- Okay AI, Tüysüz O (1999). Tethyan sutures of northern Turkey. The Mediterranean basin: Tertiary extension within the Alpine orogeny. *Geological Society, London, Special Publications* 156: 475-515.  
<https://doi.org/10.1144/GSL.SP.1999.156.01.22>
- Parlak O, Çolakoğlu A, Dönmez C, et al. (2013). Geochemistry and tectonic significance of ophiolites along the Ankara-Erzincan Suture Zone in northeastern Anatolia. In: Robertson AHF, Parlak O, Ünlügenç UC (eds.), *Geological Society, London, Special Publications* 372: 75-105.  
<https://doi.org/10.1144/SP372.7>
- Plumlee GS, Smith KS, Ficklin WH, et al. (1992). Geological and geochemical controls on the composition of mine drainages and natural drainages in mineralized areas: Proceedings, 7th International Water-Rock Interaction Conference, Park City, Utah, pp. 419-422.
- Plumlee GS, Smith KS, Montour MR, et al. (1999). Geologic controls on the composition of natural waters and mine waters draining diverse mineral-deposit types. In: Filipek LH, Plumlee GS (eds.), *The environmental geochemistry of mineral deposits. Part B: case studies and research topics*, vol 6B. Society of Economic Geologists, Littleton pp 373-432.  
<https://doi.org/10.5382/Rev.06.19>
- Plunder A, Agard P, Chopin C, et al. (2013). Geodynamics of the Tavşanlı zone, western Turkey: Insights into subduction/obduction processes. *Tectonophysics* 608: 884-903.  
<https://doi.org/10.1016/j.tecto.2013.07.028>
- Price WA, Errington J, Koyanagi V (1997). Guidelines for the prediction of acid rock drainage and metal leaching for mines in British Columbia: part I. General procedures and information requirements; In: *Proc, 4th ICARD*, Natural Resources Canada, Ottawa, 1: 1-14.
- RG (Resmi Gazete/Turkish Official Gazette) 28483 (2012). Regulation on Surface Water Quality Management, the Turkish Standards, Ankara (revision: RG-15/4/2015-29327).
- Rocscience (2019). RS2 2D geotechnical finite element software package, Rocscience Inc., Toronto, Canada.
- Rötting TS, Caraballo MA, Serrano JA, et al. (2008). Field application of calcite dispersed alkaline substrate (calcite-DAS) for passive treatment of acid mine drainage with high Al and metal concentrations. *Applied Geochemistry* 23: 1660-1674.  
<https://doi.org/10.1016/j.apgeochem.2008.02.023>
- Şaşmaz M, Akgül B, Yıldırım D, et al. (2016). Mercury uptake and phytotoxicity in terrestrial plants grown naturally in the Gümüşköy (Kütahya) mining area, Turkey. *International Journal of Phytoremediation* 18(1): 69-76.  
<https://doi.org/10.1080/15226514.2015.1058334>
- Şengör AMC, Yılmaz Y (1981). Tethyan evolution of Turkey: a plate tectonic approach. *Tectonophysics* 75: 181-241.  
[https://doi.org/10.1016/0040-1951\(81\)90275-4](https://doi.org/10.1016/0040-1951(81)90275-4)
- Şengör AMC, Görür N, Şaroğlu F (1985). Strike-slip faulting and related basin formation in zones of tectonic escape: Turkey as a case study. In: Biddle KT, Christie-Blick N (eds.), *Strike-slip deformation, basin formation and sedimentation*. Society of Economic Paleontologists and Mineralogists Special Publication 37: 227-264.  
<https://doi.org/10.2110/pec.85.37.0211>
- Singer PC, Stumm W (1970) *Acidic Mine Drainage: The rate-determining step*. *Science* 167: 1121-1123.  
<https://doi.org/10.1126/science.167.3921.1121>

- Skousen JG, Sencindiver JC, Smith RM (1987). A Review of Procedures for Surface Mining and Reclamation in Areas with Acid-Producing Materials. Natl. Res. Center for Coal and Energy, Natl. Mine Land Reclamation Center, Morgantown, WV.
- Skousen JG, Sexstone A, Ziemkiewicz PF (2000). Acid mine drainage control and treatment. In: Barnhisel RI, Darmody RG, Daniels WL (eds.), Reclamation of Drastically Disturbed Lands. Agronomy Monographs 41: 131-168. <https://doi.org/10.2134/agronmonogr41.c6>
- Smith RM, Sobek AA, Arkle T, et al. (1976). Extensive overburden potentials for soil and water quality. EPA-600/2-76-184. USEPA, Cincinnati, OH, USA.
- Sobek AA, Schuller WA, Freeman JR, et al. (1978). Field and laboratory methods applicable to overburdens and minesoils. EPA-600/2-78-054. US Govt Printing Office, Washington, DC.
- Soregaroli BA, Lawrence RW (1998). Update on waste characterisation studies. In: Proc. Mine Design, Operations and Closure conference, Polson, MT, USA.
- Tekin UK, Göncüoğlu MC, Turhan N (2002). First evidence of Late Carnian radiolarians from the Izmir-Ankara suture complex, central Sakarya, Turkey: implications for the opening age of the Izmir-Ankara branch of Neo-Tethys. *Geobios* 35: 127-135. [https://doi.org/10.1016/S0016-6995\(02\)00015-3](https://doi.org/10.1016/S0016-6995(02)00015-3)
- Vıcl M (1982). Mineralization of Gümüşköy (Kütahya) Aktepe Pb-Zn-Sb-Ag. PhD Dissertation, Aegean University. (In Turkish)
- Yaldız T (2007). Mineral enrichments effects to public health located among the Aliköy, Vakıf and Köreken (Tavşanlı-Kütahya) villages. MSc Thesis, Institute of the Natural and Applied Sciences, Selçuk University. (In Turkish)
- Yaroshevsky AA (2006). Abundances of chemical elements in the Earth's crust. *Geochemistry International* 44(1): 54-62. <https://doi.org/10.1134/S001670290601006X>
- Yiğitgüden HY (1984). Silver ore deposit located vicinity of Kütahya West Anatolia-Türkiye. PhD Dissertation, Nordrhein-Westfalen Technical High School, Dortmund, Germany.
- Yıldırım D, Şaşmaz A (2017). Phytoremediation of As, Ag, and Pb in contaminated soils using terrestrial plants grown on Gümüşköy mining area (Kütahya Turkey). *Journal of Geochemical Exploration* 182: 228-234. <https://doi.org/10.1016/j.gexplo.2016.11.005>
- Ziegler J (1960). Brief report on the barite-graphite ores vicinity of Gümüşköy-Kütahya. General Directorate of Mineral Research and Exploration of Turkey (MTA). Compilation Reports No. 448, Ankara, Turkey. pp 5-14. (In Turkish)